Synthesis and self-assembly of AB2-type amphiphilic copolymers from biobased hydroxypropyl methyl cellulose and poly(L-lactide)

Aijing Lu, Jielin Wang, Marleny Caceres Najarro, S.M. Li, André Deratani

▶ **To cite this version:**

Aijing Lu, Jielin Wang, Marleny Caceres Najarro, S.M. Li, André Deratani. Synthesis and self-assembly of AB2-type amphiphilic copolymers from biobased hydroxypropyl methyl cellulose and poly(L-lactide). Carbohydrate Polymers, 2019, 211, pp.133-140. 10.1016/j.carbpol.2019.01.110 . hal-02076331

HAL Id: hal-02076331

https://hal.umontpellier.fr/hal-02076331v1

Submitted on 21 Oct 2021

HAL is a multi-disciplinary open access archive for the deposit and dissemination of scientific research documents, whether they are published or not. The documents may come from teaching and research institutions in France or abroad, or from public or private research centers.

L'archive ouverte pluridisciplinaire **HAL**, est destinée au dépôt et à la diffusion de documents scientifiques de niveau recherche, publiés ou non, émanant des établissements d'enseignement et de recherche français ou étrangers, des laboratoires publics ou privés.

Distributed under a Creative Commons Attribution - NonCommercial 4.0 International License

Version of Record: https://www.sciencedirect.com/science/article/pii/S0144861719301249
Manuscript_3eff38cbee1d0773337d24f4f7735db6

Synthesis and Self-Assembly of AB_2-type Amphiphilic Copolymers from Biobased Hydroxypropyl Methyl Cellulose and Poly(L-lactide)

Aijing Lu, Jielin Wang, Marleny Caceres Najarro, Suming Li*, Andre Deratani

Institut Européen des Membranes, UMR CNRS 5635, Université de Montpellier, Place Eugene Bataillon, 34095 Montpellier Cedex 5, France

Abstract: AB_2-type amphiphilic $(HPMC)_2$-PLA copolymers with various hydrophilic block lengths were synthesized using a three step procedure: ring-opening polymerization of L-lactide initiated by propynol, amination reduction of the aldehyde endgroup of HPMC, and thiol-click reaction. The resulted copolymers were characterized by NMR, DOSY-NMR, SEC and FT-IR. The cloud point (CP) was determined by UV–visible spectrometer. Data show that the HPMC block length has little effect on the Cp of the copolymers which is lower than that of HPMC. The self-assembly behavior of the copolymers was investigated from DLS, TEM, and critical micelle concentration (CMC) measurements. Spherical micelles are obtained by self-assembly of copolymers in aqueous solution. The micelle size and the CMC of copolymers increase with increasing HPMC block length. It is concluded that biobased and biodegradable $(HPMC)_2$-PLA copolymers could be promising as nano-carrier of hydrophobic drugs.

* Corresponding authors: suming.li@umontpellier.fr (S. Li)

© 2019 published by Elsevier. This manuscript is made available under the CC BY NC user license
https://creativecommons.org/licenses/by-nc/4.0/

1. Introduction

Micelles based on amphiphilic block copolymers have been extensively investigated as drug carrier due to their favorable advantages in molecular design, long circulation, enhanced drug loading and therapeutic effect, and biocompatibility (Kataoka, Harada, & Nagasaki, 2001). Thus, biocompatible and bioresorbable aliphatic polyesters such as polylactide (PLA), polyglycolide (PGA), poly(lactide-co-glycolide) (PLGA), and poly(ε-caprolactone) (PCL) have been commonly used as the hydrophobic block, whereas poly(ethylene glycol) (PEG), poly(N-vinyl-2-pyrrolidone) (PVP), poly(N-isopropylacrylamide) (PNIPAAm), poly(vinyl alcohol) (PVA), poly(amino acid), and more recently polysaccharides as the hydrophilic block to construct amphiphilic block copolymers (Elsabahy & Wooley, 2012; Guo, Wang, Shen, Shu, & Sun, 2013; Mi, Wang, Nishiyama, & Cabral, 2017; Yi et al., 2018). PLA, as an FDA-approved biobased polyester, is widely used in biomedical and pharmaceutical fields in the form of drug carrier, tissue engineering scaffolds, bone fracture internal fixation devices, orthopedic screws and plates, etc, due to its good degradability, processability, and mechanical strength (Lassalle & Ferreira, 2007; Rajendra P. Pawara & Abraham J. Dombb, 2014; Ramzi A. Abd Alsaheb, 2015; Rancan et al., 2009; Saini, Arora, & Kumar, 2016; Tsuji, 2005). Interestingly, PLA stereocomplex has been used to construct colloidal systems such as mixed micelles and hydrogels for pharmaceutical applications (L. Yang, Wu, Liu, Duan, & Li, 2009).

PEG is also an FDA-approved polymer widely used for biomedical and pharmaceutical applications. Nevertheless, PEG as a polyether is prone to peroxidation, which could

adversely affect cells (Barz, Luxenhofer, Zentel, & Vicent, 2011; Ishida & Kiwada, 2008). Therefore, great effort has been made to search for hydrophilic alternatives of PEG. Polysaccharides have attracted increasing attention in recent years for uses as biomaterials to solve problems related to immunogenicity and toxicity associated with synthetic polymers because of their biodegradability, biocompatibility and bio-based nature (Aminabhavi, Nadagouda, Joshi, & More, 2014; Ganguly, Chaturvedi, More, Nadagouda, & Aminabhavi, 2014). Certain polysaccharides present inherent bioactivity that can help in mucoadhesion, thus improving drug targeting and diminishing inflammatory response. Recent years have witnessed a rapid growth on polysaccharide based micelles as drug delivery system (Aminabhavi et al., 2014; Rudzinski & Aminabhavi, 2010), such as pullulan (Jeong et al., 2006), cellulose (Guo, Wang, Shu, Shen, & Sun, 2012), dextran (Jeong et al., 2011; Sun et al., 2009), chitosan (Huo et al., 2012), heparin (Tian et al., 2010), and hyaluronan (Y. L. Yang, Kataoka, & Winnik, 2005). Among them, cellulose is of great importance because of its outstanding properties, but its applications are restrained due to its poor solubility. Thus, soluble cellulose derivatives have been studied as a hydrophilic building block to prepare amphiphilic copolymers which can self-assemble in micelles, such as ethyl cellulose, hydroxyl propyl cellulose (Ostmark, Nystrom, & Malmstrom, 2008), hydroxyl propyl methyl cellulose (HPMC) (Ostmark et al., 2008), hydroxyl ethyl cellulose (Hsieh, Van Cuong, Chen, Chen, & Yeh, 2008) etc. Graft copolymerization of PLA onto cellulose and cellulose derivatives have been reported (Chen & Sun, 2000; Teramoto & Nishio, 2003; Yuan, Yuan, Zhang, & Xie, 2007). However, the grafting of PLA on the side chain hydroxyl group results in complex chain structure and the reaction is poorly controllable.

In our previous work (Wang, Caceres, Li, & Deratani, 2017), linear HPMC-*b*-PLA diblock copolymers with various HPMC block lengths were synthesized by combination of ring-opening polymerization, amination reduction and thiol-click reaction. The resulted amphiphilic copolymers are susceptible to self-assemble into spherical micelles with a diameter of 60-120 nm. It has been shown that the geometrical structure of copolymers affect the morphology, stability and size of micelles because the hydrophobic and hydrophilic segments lead to complex spatial arrangements during the micellization process (Cao et al., 2013; Li, Kesselman, Talmon, Hillmyer, & Lodge, 2004). In this work, amphiphilic AB_2-type PLA-$(HPMC)_2$ copolymers with various HPMC molar masses were synthesized and characterized. The self-assembly properties of the copolymers were investigated from the morphology, size and size distribution, cloud point (Cp) and critical micelle concentration (CMC) measurements.

2. Materials and Methods

2.1 Materials

L-lactide was purchased from Purac Biochem (Goerinchem, Netherlands) and purified by recrystallization from ethyl acetate. HPMC (K4M) was kindly provided by Colorcon-Dow chemical (Bougival, France). Propynol, stannous octoate ($Sn(Oct)_2$), cysteamine, sodium cyanoborohydride ($NaBH_3CN$), 1,4-dithiothreito (DTT), 2,2-dimethoxy-2-phenylacetophenone (DMPA), diethyl ether and dimethyl sulfoxide were purchased from Sigma-Aldrich, and used as received. Toluene was purchased from Sigma-Aldrich, dried over by calcium chloride ($CaCl_2$) and distilled prior to use.

89 2.2 Synthesis of alkynyl terminated PLLA

90 Alkynyl terminated PLLA was synthesis by ring-open polymerization, of L-lactide using
91 propynol as initiator and $Sn(Oct)_2$ as catalyst. Typically, L-lactide (7.2 g), propynol (0.112 g),
92 and $Sn(Oct)_2$ (0.2 g) were introduced into a dried Schlenk tube, and 30 mL anhydrous toluene
93 was added under stirring. The solution was degassed by performing five freeze–pump–thaw
94 cycles. The reaction then proceeded 24 h at 80°C. Finally the product was obtained by
95 precipitation in methanol, followed by vacuum drying.

96 2.3 Enzymatic degradation of HPMC and determination of substitution degree

97 HPMC was depolymerized to yield HPMC oligomers as reported in a previous work
98 (Wang et al., 2017). Briefly, 1 g HPMC was added in 100 mL citrate phosphate buffer (pH =
99 5), and stirred overnight at 47 °C to ensure complete dissolution. Cellulase was added to the
100 solution, and enzymatic depolymerization proceeded for various time periods. The reaction
101 was stopped by heating the solution to 85 °C, and the suspension was hot filtrated. The
102 collected solution was purified by dialysis for 3 days using a membrane of MWCO=3500 g
103 mol^{-1}, followed by freeze drying.

104 HPMC is a cellulose derivative whose hydroxyl groups are substituted by methyl and
105 hydroxypropyl groups. The average number of substituents per repeat unit is characterized by
106 the molar substitution or hydroxypropylaction (MS_{HP}) and the degree of substitution or
107 methylation (DS_{Me}). The former can be higher than 3 and the latter varies between 0 and 3.
108 HPMC with a DS_{Me} between 0.1 and 2.0 is water soluble as the substitution groups allow to
109 decrease the intra- and inter-chain hydrogen bonding. In contrast, when the DS is above 2,
110 HPMC becomes insoluble in water due to the presence of many hydrophobic methyl groups.

(Claes, 2006). The ^{1}H NMR spectra of acetylated HPMC oligomers were acquired in $CDCl_3$ at 50 °C. The DS_{Me} and MS_{HP} values were then calculated according to the method reported by Fitzpatrik (Fitzpatrick et al., 2006).

2.4 Synthesis of thiol terminated HPMC

Thiol terminated HPMC was obtained by reductive amination connecting the aldehyde end group of HPMC molecules and the amine group of cysteamine in the presence of sodium cyanoborohydride. Briefly, HPMC with DS_{Me} of 1.43 and average molar mass of 7000 g mol^{-1} (1 g) and $NaBH_3CN$ (0.2 g) were solubilized in a mixture (3/1 v/v) of 50 mL dimethyl sulfoxide (DMSO) and 0.01 M NaCl at 60 °C. Cysteamine (0.1 g) was added, and the solution was stirred at 60 °C for 6 days under reflux. The solution was then dialyzed against deionized water for 3 days (MWCO 3500 g mol^{-1}), followed by freeze drying. Afterwards, the product was dissolved in water, and stirred overnight in the presence of excess DTT under nitrogen atmosphere. Finally, the solution was dialyzed against deionized water and freeze dried. Ellman assay was performed to determine the content of thiol group using 5,5'-dithio-bis-(2-nitrobenzoic acid) (DTNB) as Ellman's reagent. DTNB is a versatile water soluble compound for quantitating free sulfhydryl groups as a measurable yellow-colored product is formed when DTNB reacts with sulfhydryl in solution.

2.5 Synthesis of $(HPMC)_2$-*b*-PLLA

Amphiphilic block copolymers were synthesized by thiol-yne click reaction connecting thiol terminated HPMC and alkynyl terminated PLLA. The reaction was initiated in a Dinics M3 UV chamber equipped with a PL-L 36 W/01/4P Hg Lamp. Typically, thiol terminated

HPMC (1.0 g), alkynyl terminated PLLA (0.15 g), and DMPA (0.013 g) were dissolved in 10 mL DMSO. The solution was degassed for 30 min using purified argon, and then subjected to UV irradiation for 5 h. The crude product was collected by precipitation in acetonitrile, followed by centrifugation at 4500 rpm for 15 min. The above dissolution–precipitation cycle was repeated twice. Finally, $(HPMC)_2$-*b*-PLLA copolymers were obtained as a white solid after vacuum drying.

2.6 Characterization

^1H NMR spectra were recorded on Bruker spectrometer operating at 300 MHz (AMX300) using $CDCl_3$ and DMSO-d_6 as solvent. Diffusion ordered spectroscopy (DOSY) NMR was performed on Bruker Avance (AQS600) NMR spectrometer, operating at 600 MHz and equipped with a Bruker multinuclear z-gradient inverse probe head which is able to produce gradients in the z direction with the strength of 55 Gcm^{-1}. The DOSY spectra were acquired from Bruker topspin software (version 2.1) with the ledbpgp2s pulse program. The strength of the pulsed field gradients with respect to maximum 32 increments on a quadratic scale was logarithmically incremented from 2 to 95%. The diffusion sensitive period (Δ) of 200 ms and the gradient duration (δ) of 5 ms were optimized to allow the signals of interest to decrease by a factor of 10–20, in order to keep the relaxation contribution to the signal attenuation constant and ensure full signal attenuation for all samples. Data were processed using the MestRe Nova software.

Size exclusion chromatography (SEC), equipped with MALLS in combination with refractive index (RI) detection allows to determine the absolute molar mass of polymers. 5 mg of samples were added in the mobile phase (0.01 M NaCl containing 0.02% NaN_3), and

stirred for 24 h at room temperature. The solution was filtered using 0.45 µm polytetrafluoroethylene (PTFE) filter (Millipore). The filtrate was injected through a 100 µL loop (Rheodyne injector 7725), and eluted on a TSK-GEL GMPWXL 7.8×300 mm column (TosoHaas Bioseparation Specialists, Stuttgart, Germany) at a flow rate of 0.5 mL min^{-1} (Waters pump 515). MALS detector (Dawn DSP, Wyatt Technology Co, Santa Barbara, CA, USA) and RI detector (Optilab Wyatt Technology Co) were used to online determine the absolute molar mass for each elution fraction of 0.01 mL, which enables to calculate the weight average molar mass (M_w) and the dispersity ($Đ=M_w/M_n$). The refractive index increment (dn/dc) for calculation was 0.137 mL g^{-1}. Data analysis was realized using Astra 4 (Wyatt Technology Co).

Fourier transform infrared (FT-IR) spectra were recorded on a Nicolet NEXUS spectrometer with a DTGS detector at 4 cm^{-1} resolution. 64 scans were taken per sample in the frequency range from 400 to 4000 cm^{-1}. Sample pellets were prepared by mixing 2–2.5 mg of polymer with 200 mg of spectral grade potassium bromide, followed by compression using a press.

The cloud point (Cp) of the copolymers was estimated from transmittance changes of copolymer solutions in the temperature range from 30 to 90°C. The solution at 3.0 mg mL^{-1} was stirred for 24 h and kept at 5 °C overnight before analysis. Measurements were made at a wavelength of 600 nm with a Perkin Elmer Lambda 35 UV–visible spectrometer equipped with a Peltier temperature programmer PTP-1+1. The temperature ramp was 0.1 °C min^{-1}. Temp Lab software was used for data treatment.

Dynamic light scattering (DLS) was performed at 25°C with 90° scattering angle using

Zano-ZS (Malvern Instrument) equipped with a He–Ne laser (λ =632.8 nm). The aqueous solutions of copolymers at 1.0 mg mL^{-1} were filtered through a 0.45 μm PTFE microfilter before measurements. The correlation of the distribution of diffusion coefficient (D) was analyzed via the general purpose method (non-negative least squares). The apparent equivalent hydrodynamic radius (R_H) was obtained using the cumulate method from the Stoke–Einstein equation.

The critical micelle concentration (CMC) of copolymers was determined using an autocorrelation function according to the methodology proposed by Muller et al (Muller et al., 2015). Aqueous solutions of copolymers were prepared in deionized water at concentrations ranging from 0.006 to 1.0 g L^{-1}, and were incubated overnight. The scattering intensity of the solutions was measured at 25 °C with a Malvern Instrument Nano-ZS. The scattering intensity proportional to the size and number of objects present in the solution was recorded. The CMC was taken as the intersection of regression lines from the plots of the scattering intensity against the polymer concentration.

Transmission electron microscopy (TEM) was performed on JEOL 1200 EXII instrument, operating at an acceleration voltage of 120 kV. 5 μL of micellar solution at 1.0 mg mL^{-1} were dropped onto a carbon coated copper grid, and air dried before measurements.

3. Results and Discuss

3.1 Synthesis of amphiphilic block copolymers

HPMC was depolymerized by using cellulase to yield oligomers with various molar masses. The weight average molar mass (M_w) of the resulted HPMC oligomers was 5000,

7000 and 10000 Daltons, respectively, as determined by SEC. The NMR spectra of acetylated HPMC were recorded in $CDCl_3$ (Figure S1). The DS_{Me} and MS_{HP} were calculated according to the method reported by Fitzpatrik (Table S1). The DS_{Me} varies from 1.17 to 1.43, indicating that HPMC samples are water soluble.

The synthesis of $(HPMC)_2$-*b*-PLA copolymers was achieved in three steps (Scheme 1): a) synthesis of alkynyl terminated PLLA, b) thiolation of HPMC, and c) UV-initiated thiol-yne click reaction between thiolated HPMC and alkynyl terminated PLLA.

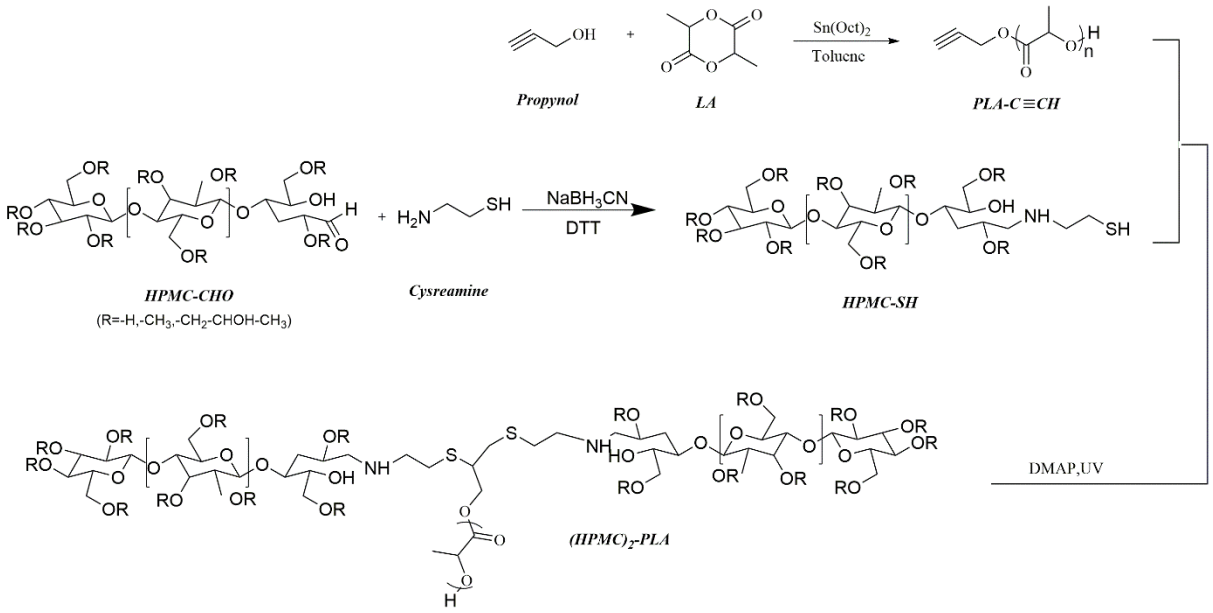

Scheme 1. Synthesis route of $(HPMC)_2$-*b*-PLA block copolymers

Alkynyl terminated PLLA was synthesized by ring-opening polymerization of L-lactide using propynol as initiator with a monomer/initiator molar ratio of 25/1. Figure 1 shows the ^1H NMR spectrum of the resulting alkynyl terminated PLLA. The signals at 2.4 (**a**) and 4.75 (**b**) ppm are assigned to the alkynyl group and the methylene groups adjacent to the alkynyl group, respectively. The signals at 1.62 (**d**) and 5.25 (**c**) ppm are assigned to the methyl and

methyne protons of PLA main chain, and the signals at 1.50 (**f**) and 4.42 (**e**) ppm to methyl and methyne protons of the hydroxyl terminal unit. The polymerization degree (DP) of PLA calculated from the integration ratio of signals **c** to **e** was 28, corresponding to a number average molar mass ($M_{n,NMR}$) of about 2000 g/mol.

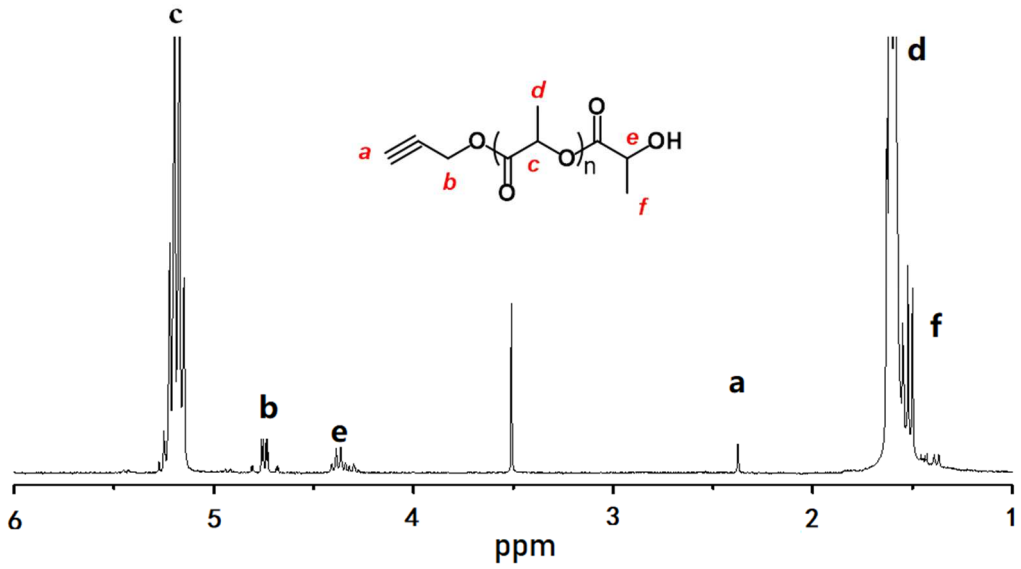

Figure 1. NMR spectrum of alkynyl–terminated PLA in $CDCl_3$

Thiol terminated HPMC was obtained by reductive amination of HPMC with cysteamine. The molecular chain of cellulose has a non reducing group at one end, and a hemiacetal group at the other end. The latter is a reducing group which can be easily converted to aldehyde group (Schatz & Lecommandoux, 2010). The amine functional group of cysteamine reacted with the unique aldehyde endgroup of HPMC through reductive amination to yield HPMC-S-S-HPMC together with small amounts of unreacted HPMC, HPMC-SH, and HPMC-S-S-$(CH_2)_6$-NH_2. HPMC-S-S-HPMC was then reduced using DTT to yield HPMC-SH (Wang et al., 2017). The final product was characterized by using Ellman assay and SEC measurement. Ellman's assay showed that the content of thiol terminated

231 HPMC in the final product was 88%. SEC confirmed that the final product is predominantly
232 composed of HPMC-SH because its M_w is almost the same as that of the initial HPMC. These
233 findings showed that thiol terminated HPMC was successful synthesized.

234 Finally amphiphilic block copolymers were obtained by UV-initiated thiol-yne click
235 reaction between thiol terminated HPMC and alkynyl terminated PLLA. Three copolymers,
236 namely $(HPMC5K)_2$-PLA2K, $(HPMC7K)_2$-PLA2K and $(HPMC10K)_2$-PLA2K were
237 synthesized using the same hydrophobic PLA block with M_n of 2000 g mol^{-1} and different
238 hydrophilic HPMC-SH blocks with M_w of 5000, 7000, and 10000 g mol^{-1}, respectively.
239 Figure 2 shows the ^1H NMR spectra of $(HPMC7K)_2$-PLA2K copolymer in D_2O and DMSO-
240 *d_6*. The spectrum in DMSO-*d_6* shows the signal at 1.05 ppm (a) corresponding to the methyl
241 protons in the hydroxypropyl group, and those in the range of 2.75–4.75 ppm (b) to the
242 methyl protons adjacent to the oxygen moieties of the ether linkages, inner methylene and
243 methine protons and HPMC backbone protons (Figure 2A). The signals at 1.49 (d) and 5.24
244 ppm (c) belong to the methyl and methine protons of PLLA blocks. Moreover, the signal
245 detected at 2.3 ppm is assigned to the methylene group of the connecting unit. These results
246 confirm the successful synthesis of copolymers by thiol-yne click reaction.

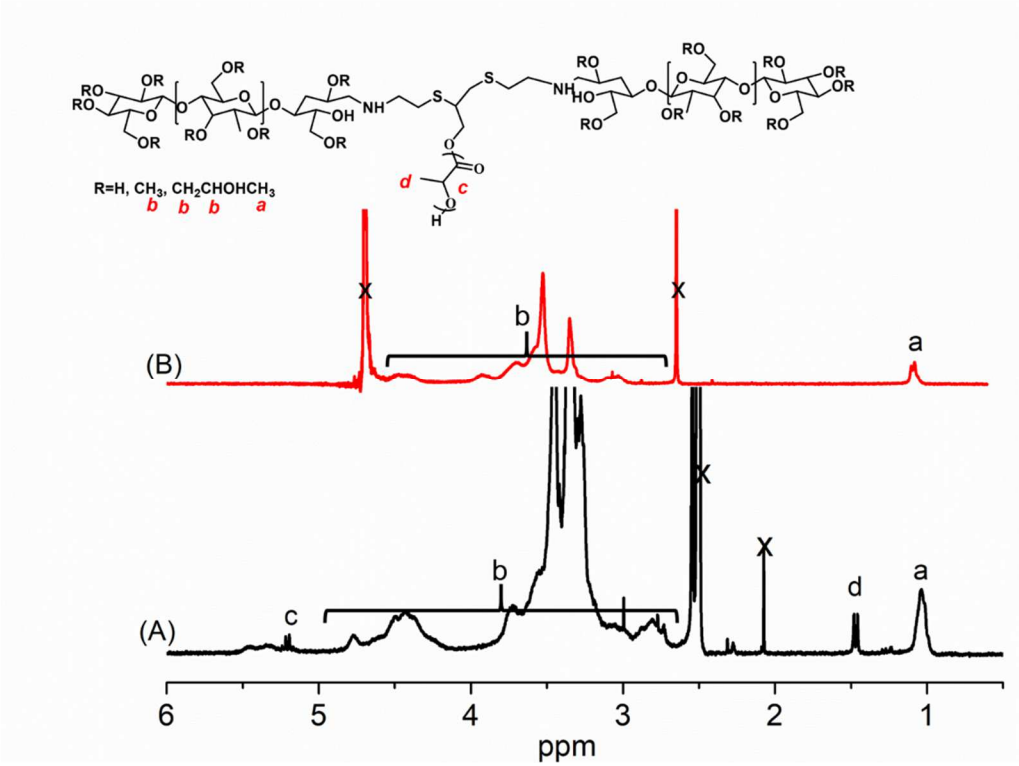

Figure 2. ^{1}H NMR spectra of $(HPMC)_2$-PLA in DMSO-d_6 (A) and in D_2O (B)

The structure of block copolymers was also confirmed by DOSY-NMR. DOSY is an excellent tool commonly used for the analysis of complex mixtures as it allows virtual separation of multicomponent systems. DOSY-NMR data are presented in a two-dimensional (2D) pattern: one dimension is related to the chemical shift information, and the other represents the diffusion coefficient which reflects the molecular effective sizes (Pages, Gilard, Martino, & Malet-Martino, 2017). As shown in Figure 3, the signals of both PLA and HPMC components present the same diffusion coefficient, which indicates that the two blocks are attached in one molecule. In other words, the copolymer was effectively synthesized.

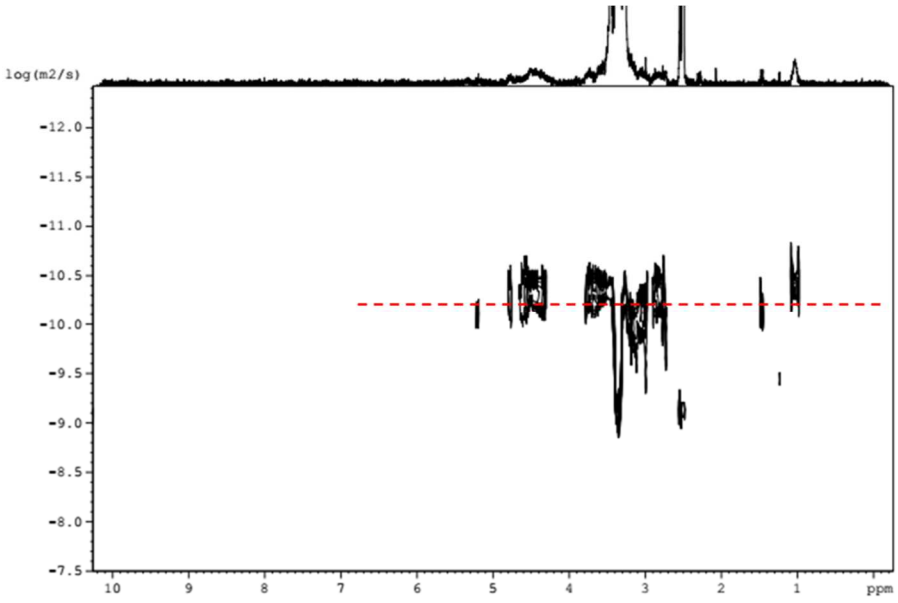

Figure 3. DOSY NMR spectrum of $(HPMC7K)_2$-PLA2K copolymer in DMSO-d_6 at 298 K

FT-IR is also used to examine the structure of copolymers. Figure 4 presents the FT-IR spectra of alkynyl terminated PLLA, thiol terminated HPMC, and $(HPMC7K)_2$-PLA2K copolymer. Alkynyl terminated PLLA presents characteristic absorption bands at 1760, 2130 and 3300 cm^{-1} belonging to the carbonyl group, and alkynyl group, respectively. Thiol terminated HPMC presents an amide adsorption band at 1652 cm^{-1}, a strong C-O absorption band at 1047 cm^{-1}, and a broad O-H stretching vibration band at 3480 cm^{-1}. $(HPMC)_2$-b-PLA shows the characteristic bands from both components, in agreement with the successful coupling of PLLA and HPMC blocks.

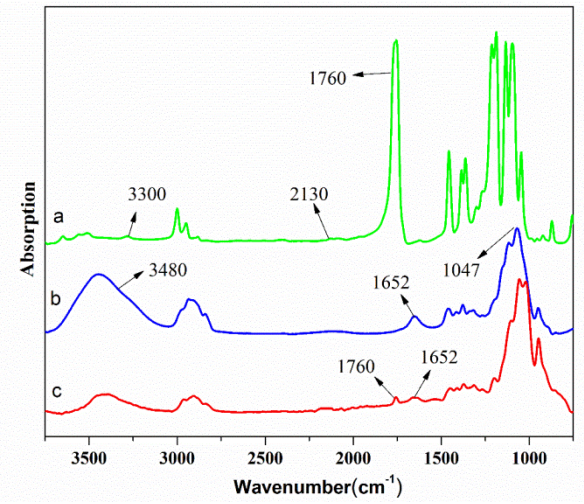

Figure 4. FT-IR spectra of (a) alkynyl terminated PLLA, (b) thiol terminated HPMC, and (c) $(HPMC7K)_2$-PLA2K copolymer.

The molar mass of the copolymers was determined by SEC in conjunction with online light scattering and refractive index (RI) detectors, as shown in Figure 5. RI detector is most commonly used as concentration detector whose response is proportional to the total solute concentration in the detector cell. Meanwhile, the response of multi-angle laser light scattering (MALLS) detector depends on the molar mass of a polymer in the detector cell (Kostanski, Keller, & Hamielec, 2004). Combination of the two curves allows to determine the weight average molar mass of copolymers.

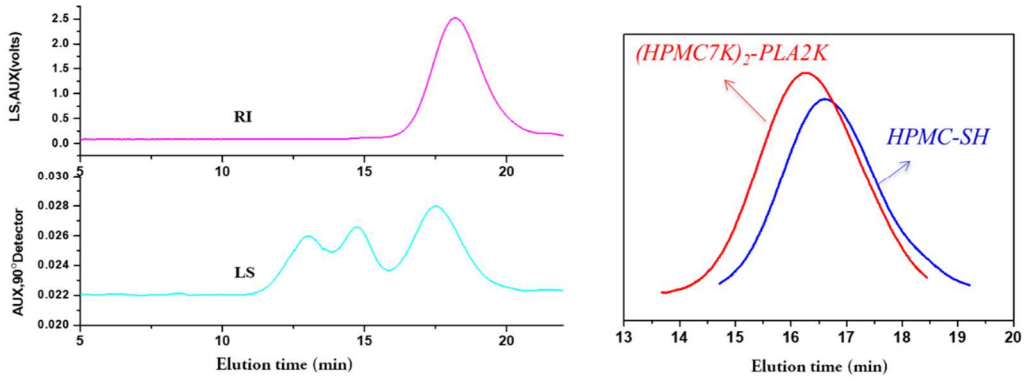

Figure 5. Refractive index and light scattering curves of $(HPMC7K)_2$-PLA2K (left), and SEC curves of HPMC-SH and $(HPMC7K)_2$-PLA2K in water

The M_w and dispersity data of the three copolymers are summarized in Table 1. The M_w ranges from 12000 for $(HPMC5K)_2$-PLA2K to 22 0000 g mol^{-1} for $(HPMC10K)_2$-PLA2K. It is noted that the M_w of the copolymers well agrees with the sum of the molar masses of both components although the value of M_n is used for PLA. Meanwhile, the dispersity ($Đ=M_w/M_n$) ranges from 1.13 to 1.26, in agreement with narrow molar mass distribution of copolymers.

Table 1. Characterization of $(HPMC)_2$-PLA copolymers

Sample	$M_{w, SEC}$ [a] (g/mol)	Đ [a]	Cp [b] (°C)	CMC [c] (mg/mL)	R_h [d] (nm)	PDI [d]
$(HPMC10K)_2$-PLA2K	22000	1.26	65.2	0.16	120	0.21
$(HPMC7K)_2$-PLA2K	16000	1.24	64.8	0.15	90	0.12
$(HPMC5K)_2$-PLA2K	12000	1.13	64.1	0.14	66	0.19

[a] Determined from SEC/MALS/RI measurement in water at 5.0mg mL^{-1}
[b] Determined from turbidimetry measurement in water at 20.0 mg mL^{-1}
[c] Determined at 25°C by dynamic light scattering
[d] Determined at 25°C by dynamic light scattering at 1.0 mg mL^{-1}

3.2. Cloud point of $(HPMC)_2$-PLA copolymers

The cloud point (Cp), also named lower critical solution temperature (LCST), is considered as the solubility limit of amphiphiles due to phase-separation as the temperature increases. In fact, the hydrogen bonding between polymer chains and surrounding water

molecules weakens when the temperature approaches the cloud point, leading to decrease of the polymer solubility and phase separation. Thus the polymer precipitates out of solution as a consequence of equal chemical potentials between the two phases: one is rich in polymer, and the other rich in solvent (Sardar, Kamil, Kabir ud, & Sajid Ali, 2011).

Figure 6 shows the transmittance changes of $(HPMC7K)_2$-PLA2K solutions at 3.0 mg/mL, in comparison with HPMC7K homopolymer. The two solutions initially exhibit a transmittance close to 100%. With increasing temperature, the transmittance of HPMC7K remained almost unchanged till 90°C. This indicates that HPMC oligomers are not thermos-responsive in this temperature range, in contrast to high molar mass HPMC (Sardar et al., 2011). Interestingly, $(HPMC7K)_2$-PLA2K exhibits a decrease of light transmittance to nearly 20% from about 60°C up to 90 °C. The clouding at a given temperature results from the destruction of hydrogen bonding between water and HPMC molecules leading to phase separation (Khan, Anjum, Koya, Qadeer, & Kabir ud, 2014). The Cp value was determined by extrapolation of the linear region of 100% of transmittance and tangent line of the inflexion point. A Cp value of 64.8°C is obtained for $(HPMC7K)_2$-PLA2K. Similarly, Cp values of 65.2 and 64.1°C are obtained for $(HPMC10K)_2$-PLA2K and $(HPMC5K)_2$-PLA2K (Table 1). Therefore, the length of HPMC blocks has little effect on the Cp value of the copolymers. Similar results have been previously reported in literature for poly(lactide-*b*-*N*-isopropylacrylamide-*b*-lactide) (PLA-*b*-PNIPAAm- *b*-PLA) triblock copolymers (You, Hong, Wang, Lu, & Pan, 2004). In fact, a Cp value of about 31°C was obtained for copolymers with PLA/PNIPAAm ratios of 1.0/1.9, 1.0/3.0 and 1.0/3.6.

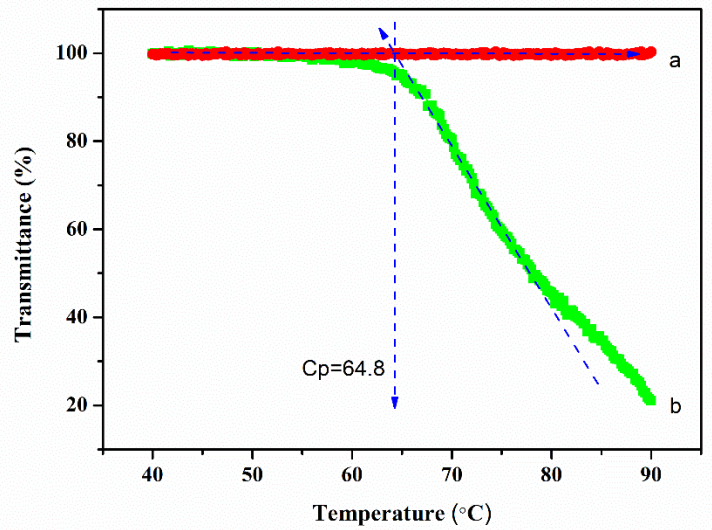

Figure 6. Transmittance changes of HPMC7K (a) and $(HPMC7K)_2$-PLA2K (b) solutions at 3.0 mg/mL as a function of temperature.

In our previous work, the phase separation behavior of linear HPMC-*b*-PLA diblock copolymers with different HPMC block lengths (HPMC5K-PLA2K, HPMC8K-PLA2K, and HPMC10K-PLA2K) was investigated (Wang et al., 2017). All copolymers exhibit a slow decrease of light transmittance from 55 to 80 °C. Beyond, a sharper decrease of transmittance down to 78% is detected. The three diblock copolymers exhibit almost the same Cp values of *c.a.* 80°C. Therefore, the length of HPMC blocks has little effect on the Cp, but the copolymer topology seems to significantly affect the phase separation behavior of HPMC-*b*-PLA copolymers. It has been reported that the cloud point was elevated by more than 40 °C through the linear-to-cyclic topological conversion of the polymer amphiphiles (Honda, Yamamoto, & Tezuka, 2010).

3.3. Self-assembly of $(HPMC)_2$-PLA copolymers

The self-assembly properties of $(HPMC)_2$-PLA copolymers were investigated to evaluate

their potential as drug carrier. NMR provides a means to analyze the self-assembly behavior of amphiphilic block copolymers in solvents which can dissolve one of the two blocks only. Figure 2(B) shows the ^{1}H NMR spectrum of $(HPMC7K)_2$-PLA2K copolymer in deuterated water (D_2O). Different from DMSO-*d*$_6$ which is a good solvent for both HPMC and PLLA, D_2O only solubilizes hydrophilic HPMC segments. Therefore, only signals belonging to HPMC block are detected. Signals corresponding to PLLA block are not detected because of the limited molecular motion in aqueous medium, which is consistent with the formation of micelles with a hydrophilic HPMC shell and a hydrophobic PLLA core.

Similar to low molar mass surfactants, the self-assembly of the amphiphilic copolymers occurs when the concentration reaches the CMC. The latter is an important parameter of amphiphilic copolymers as it determines the stability of micelles. In the case of drug delivery systems, drug loaded micelles should remain stable with dilution after intravenous injection. In this work, the CMC was determined from scattering intensity changes of copolymer solutions as a function of concentration. At low concentrations, the scattered intensity is very low because of the absence of nano-objects. With increasing concentration, the intensity strongly increases due to the formation of nano-micelles. The CMC value is obtained from the crossover point of the two regression lines. As shown in Table 1, the CMC of $(HPMC10K)_2$-PLA2K, $(HPMC7K)_2$-PLA2K, and $(HPMC5K)_2$-PLA2K copolymers is 0.16, 0.15, and 0.14 g L^{-1}, respectively. These values well agree with the reported CMC value 0.13 mg/mL for cellulose-*g*-polylactide (Guo et al., 2012). Obviously the CMC increases with the hydrophilic ratio or the HPMC block length as the self-assembly of neutral block copolymers is mainly determined by the hydrophilic/hydrophobic balance (Larue et al., 2008).

363 The self-assembled $(HPMC)_2$-PLA micelles are composed of a PLA core surrounded by
364 a HPMC corona. The average diameter of $(HPMC5K)_2$-PLA2K, $(HPMC7K)_2$-PLA2K,
365 $(HPMC10K)_2$-PLA2K micelles was 66, 90 and 120 as determined by DLS, as shown in Table
366 1. All the micelles exhibited a unimodal size distribution, and the PDI was in the range of 0.12
367 to 0.21. Thus, the micelle size of copolymers increases with the increase of hydrophilic
368 HPMC chain length, in agreement with literature. In our previous work, the average micelle
369 size of HPMC5K-PLA2K, HPMC8K-PLA2K, HPMC10K-PLA2K diblock copolymers was
370 62, 96, 120 nm, respectively (Wang et al., 2017). Thus, micelles of $(HPMC5K)_2$-PLA2K had
371 a smaller size compared to HPMC10K-PLA2K with the same hydrophilic/hydrophobic
372 balance but a Y-type topology. It has been reported that the chain architecture affects the
373 micellization properties, including the aggregation number, size, polydispersity, and micelle
374 density (Liu et al., 2007). Generally, the micelle size of multiple-arm copolymers is smaller
375 than that of linear ones. Meanwhile, micelles with the same HPMC block length but different
376 topologies had almost the same size. This finding could be attributed to the fact that the core
377 is composed of the same PLA blocks, and the corona of similar HPMC chains although the
378 chain density should be higher for Y-type copolymers.
379

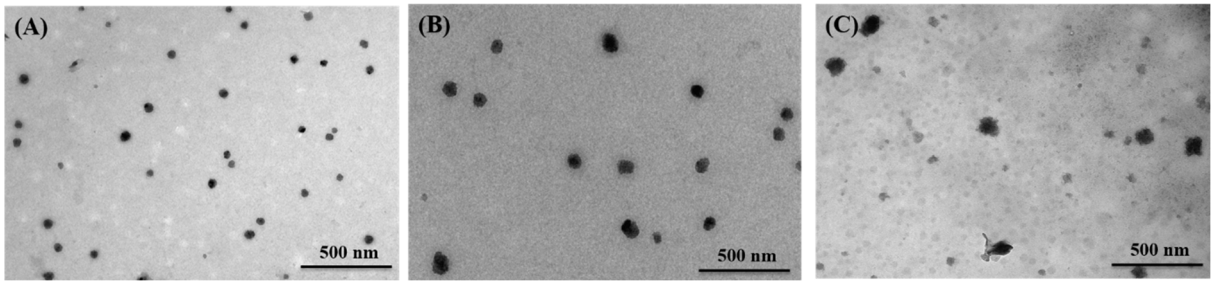

380
381 Figure 7. TEM images of $(HPMC)_2$-PLA micelles in water: (A) $(HPMC5K)_2$-PLA2K; (B)
382 $(HPMC7K)_2$-PLA2K; (C) $(HPMC10K)_2$-PLA2K.

The morphology of $(HPMC)_2$-PLA micelles was characterized by using TEM. Figure 7 shows that the micelles were spherical in shape and uniformly distributed. The observed micelle size increased with the increasing of the HPMC chain length, which well agreed with the results obtained by DLS.

4. Conclusion

AB_2-type amphiphilic block copolymers $(HPMC)_2$-PLA with three different HPMC block lengths were synthesized by ring opening polymerization, reductive amination and click reaction. The copolymers were characterized by using various methods, including NMR, DOSY-NMR, SEC and FT-IR. The cloud point of AB_2-type $(HPMC)_2$-PLA are nearly 64 ℃, which is obviously lower than HPMC oligomers and linear HPMC-b-PLA diblock copolymers. The HPMC block length has little effect the Cp value. $(HPMC)_2$-PLA copolymers can self-assemble to form spherical micelles with narrow distribution. The size of copolymer micelles increases with the increase of HPMC fraction. So does the CMC of $(HPMC)_2$-PLA. It is thus concluded that biobased and biodegradable HPMC-PLA copolymers could be promising as nano-carrier of hydrophobic drugs.

Keywords: Hydroxypropyl methyl cellulose; Poly(L-lactide); Topology; Self-assembly; Micelle

Acknowledgements

405 This work is supported in part by the scholarship from China Scholarship Council (CSC)
406 under the Grant CSC N°201606240124.

407

408 ## References

409 Aminabhavi, T. M., Nadagouda, M. N., Joshi, S. D., & More, U. A. (2014). Guar gum as platform for the oral
410 controlled release of therapeutics. *Expert Opin Drug Deliv,* 11(5), 753-766.
411 Barz, M., Luxenhofer, R., Zentel, R., & Vicent, M. J. (2011). Overcoming the PEG-addiction: well-defined
412 alternatives to PEG, from structure–property relationships to better defined therapeutics.
413 *Polymer Chemistry,* 2(9), 1900.
414 Cao, J., Lu, A., Li, C., Cai, M., Chen, Y., Li, S., & Luo, X. (2013). Effect of architecture on the micellar
415 properties of poly (varepsilon-caprolactone) containing sulfobetaines. *Colloids Surf B*
416 *Biointerfaces,* 112, 35-41.
417 Chen, D., & Sun, B. (2000). New tissue engineering material copolymers of derivatives of cellulose and
418 lactide: their synthesis and characterization. *Materials Science and Engineering: C,* 11(1), 57-60.
419 Claes, M. (2006). New Methods for Enzyme Hydrolysis,Analysis, and Characterization of Modified
420 Cellulose. *Analytical Chemistry* (Vol. Ph.D, p. 180). Lund: Lund University.
421 Elsabahy, M., & Wooley, K. L. (2012). Design of polymeric nanoparticles for biomedical delivery
422 applications. *Chem Soc Rev,* 41(7), 2545-2561.
423 Fitzpatrick, F., Schagerlöf, H., Andersson, T., Richardson, S., Tjerneld, F., Wahlund, K.-G., & Wittgren, B.
424 (2006). NMR, Cloud-Point Measurements and Enzymatic Depolymerization: Complementary Tools
425 to Investigate Substituent Patterns in Modified Celluloses. *Biomacromolecules,* 7(10), 2909-2917.
426 Ganguly, K., Chaturvedi, K., More, U. A., Nadagouda, M. N., & Aminabhavi, T. M. (2014). Polysaccharide-
427 based micro/nanohydrogels for delivering macromolecular therapeutics. *J Control Release,* 193,
428 162-173.
429 Guo, Y., Wang, X., Shen, Z., Shu, X., & Sun, R. (2013). Preparation of cellulose-graft-poly(varepsilon-
430 caprolactone) nanomicelles by homogeneous ROP in ionic liquid. *Carbohydr Polym,* 92(1), 77-83.
431 Guo, Y., Wang, X., Shu, X., Shen, Z., & Sun, R. C. (2012). Self-assembly and paclitaxel loading capacity of
432 cellulose-graft-poly(lactide) nanomicelles. *J Agric Food Chem,* 60(15), 3900-3908.
433 Honda, S., Yamamoto, T., & Tezuka, Y. (2010). Topology-directed control on thermal stability: micelles
434 formed from linear and cyclized amphiphilic block copolymers. *J Am Chem Soc,* 132(30), 10251-
435 10253.
436 Hsieh, M.-F., Van Cuong, N., Chen, C.-H., Chen, Y. T., & Yeh, J.-M. (2008). Nano-Sized Micelles of Block
437 Copolymers of Methoxy Poly(ethylene glycol)-Poly(<I>ε</I>-caprolactone)-<I>Graft</I>-2-
438 Hydroxyethyl Cellulose for Doxorubicin Delivery. *Journal of Nanoscience and Nanotechnology,*
439 8(5), 2362-2368.
440 Huo, M., Zou, A., Yao, C., Zhang, Y., Zhou, J., Wang, J., . . . Zhang, Q. (2012). Somatostatin receptor-
441 mediated tumor-targeting drug delivery using octreotide-PEG-deoxycholic acid conjugate-
442 modified N-deoxycholic acid-O, N-hydroxyethylation chitosan micelles. *Biomaterials,* 33(27),
443 6393-6407.
444 Ishida, T., & Kiwada, H. (2008). Accelerated blood clearance (ABC) phenomenon upon repeated injection

445 of PEGylated liposomes. *Int J Pharm,* 354(1-2), 56-62.
446 Jeong, Y. I., Kim, D. H., Chung, C. W., Yoo, J. J., Choi, K. H., Kim, C. H., . . . Kang, D. H. (2011). Doxorubicin-
447 incorporated polymeric micelles composed of dextran-b-poly(DL-lactide-co-glycolide) copolymer.
448 *Int J Nanomedicine,* 6, 1415-1427.
449 Jeong, Y. I., Na, H. S., Oh, J. S., Choi, K. C., Song, C. E., & Lee, H. C. (2006). Adriamycin release from self-
450 assembling nanospheres of poly(DL-lactide-co-glycolide)-grafted pullulan. *Int J Pharm,* 322(1-2),
451 154-160.
452 Kataoka, K., Harada, A., & Nagasaki, Y. (2001). Block copolymer micelles for drug delivery: design,
453 characterization and biological significance. *Adv Drug Deliv Rev,* 47(1), 113-131.
454 Khan, I. A., Anjum, K., Koya, P. A., Qadeer, A., & Kabir ud, D. (2014). Cloud point, fluorimetric and 1H NMR
455 studies of ibuprofen-polymer systems. *Journal of Molecular Structure,* 1056-1057, 254-261.
456 Kostanski, L. K., Keller, D. M., & Hamielec, A. E. (2004). Size-exclusion chromatography-a review of
457 calibration methodologies. *J Biochem Biophys Methods,* 58(2), 159-186.
458 Larue, I., Adam, M., Zhulina, E. B., Rubinstein, M., Pitsikalis, M., Hadjichristidis, N., . . . Sheiko, S. S. (2008).
459 Effect of the soluble block size on spherical diblock copolymer micelles. *Macromolecules,* 41(17),
460 6555-6563.
461 Lassalle, V., & Ferreira, M. L. (2007). PLA nano- and microparticles for drug delivery: an overview of the
462 methods of preparation. *Macromol Biosci,* 7(6), 767-783.
463 Li, Z., Kesselman, E., Talmon, Y., Hillmyer, M. A., & Lodge, T. P. (2004). Multicompartment micelles from
464 ABC miktoarm stars in water. *Science,* 306(5693), 98-101.
465 Liu, H., Xu, J., Jiang, J., Yin, J., Narain, R., Cai, Y., & Liu, S. (2007). Syntheses and micellar properties of well-
466 defined amphiphilic AB2 and A2B Y-shaped miktoarm star copolymers of ε-caprolactone and 2-
467 (dimethylamino)ethyl methacrylate. *Journal of Polymer Science Part A: Polymer Chemistry,* 45(8),
468 1446-1462.
469 Mi, P., Wang, F., Nishiyama, N., & Cabral, H. (2017). Molecular Cancer Imaging with Polymeric
470 Nanoassemblies: From Tumor Detection to Theranostics. *Macromol Biosci,* 17(1).
471 Muller, J., Marchandeau, F., Prelot, B., Zajac, J., Robin, J.-J., & Monge, S. (2015). Self-organization in water
472 of well-defined amphiphilic poly(vinyl acetate)-b-poly(vinyl alcohol) diblock copolymers. *Polymer*
473 *Chemistry,* 6(16), 3063-3073.
474 Ostmark, E., Nystrom, D., & Malmstrom, E. (2008). Unimolecular nanocontainers prepared by ROP and
475 subsequent ATRP from hydroxypropylcellulose. *Macromolecules,* 41(12), 4405-4415.
476 Pages, G., Gilard, V., Martino, R., & Malet-Martino, M. (2017). Pulsed-field gradient nuclear magnetic
477 resonance measurements (PFG NMR) for diffusion ordered spectroscopy (DOSY) mapping.
478 *Analyst,* 142(20), 3771-3796.
479 Rajendra P. Pawara, S. U. T., Suresh U. Shisodiaa, Jalinder T. Totrea and, & Abraham J. Dombb. (2014).
480 Biomedical Applications of Poly(Lactic Acid). *Recent Patents on Regenerative Medicine,* 4, 40-51.
481 Ramzi A. Abd Alsaheb, A. A., Nor Zalina Othman, Roslinda Abd Malek,Ong Mei Leng, Ramlan Aziz1 and
482 Hesham A. El Enshasy. (2015). Recent applications of polylactic acid in pharmaceutical and
483 medical industries. *Journal of Chemical and Pharmaceutical Research,* 7(12), 51-63.
484 Rancan, F., Papakostas, D., Hadam, S., Hackbarth, S., Delair, T., Primard, C., . . . Vogt, A. (2009).
485 Investigation of Polylactic Acid (PLA) Nanoparticles as Drug Delivery Systems for Local
486 Dermatotherapy. *Pharmaceutical Research,* 26(8), 2027-2036.
487 Rudzinski, W. E., & Aminabhavi, T. M. (2010). Chitosan as a carrier for targeted delivery of small interfering
488 RNA. *Int J Pharm,* 399(1-2), 1-11.

Saini, P., Arora, M., & Kumar, M. (2016). Poly(lactic acid) blends in biomedical applications. *Adv Drug Deliv Rev,* 107, 47-59.

Sardar, N., Kamil, M., Kabir ud, D., & Sajid Ali, M. (2011). Solution Behavior of Nonionic Polymer Hydroxypropylmethyl Cellulose: Effect of Salts on the Energetics at the Cloud Point. *Journal of Chemical & Engineering Data,* 56(4), 984-987.

Schatz, C., & Lecommandoux, S. (2010). Polysaccharide-Containing Block Copolymers: Synthesis, Properties and Applications of an Emerging Family of Glycoconjugates. *Macromolecular Rapid Communications,* 31(19), 1664-1684.

Sun, H., Guo, B., Cheng, R., Meng, F., Liu, H., & Zhong, Z. (2009). Biodegradable micelles with sheddable poly(ethylene glycol) shells for triggered intracellular release of doxorubicin. *Biomaterials,* 30(31), 6358-6366.

Teramoto, Y., & Nishio, Y. (2003). Cellulose diacetate-graft-poly(lactic acid)s: synthesis of wide-ranging compositions and their thermal and mechanical properties. *Polymer,* 44(9), 2701-2709.

Tian, J. L., Zhao, Y. Z., Jin, Z., Lu, C. T., Tang, Q. Q., Xiang, Q., . . . Zhang, Y. (2010). Synthesis and characterization of Poloxamer 188-grafted heparin copolymer. *Drug Dev Ind Pharm,* 36(7), 832-838.

Tsuji, H. (2005). Poly(lactide) stereocomplexes: formation, structure, properties, degradation, and applications. *Macromol Biosci,* 5(7), 569-597.

Wang, J., Caceres, M., Li, S., & Deratani, A. (2017). Synthesis and Self-Assembly of Amphiphilic Block Copolymers from Biobased Hydroxypropyl Methyl Cellulose and Poly(l
-lactide). *Macromolecular Chemistry and Physics,* 218(10), 1600558.

Yang, L., Wu, X., Liu, F., Duan, Y., & Li, S. (2009). Novel biodegradable polylactide/poly(ethylene glycol) micelles prepared by direct dissolution method for controlled delivery of anticancer drugs. *Pharm Res,* 26(10), 2332-2342.

Yang, Y. L., Kataoka, K., & Winnik, F. M. (2005). Synthesis of diblock copolymers consisting of hyaluronan and poly(2-ethyl-2-oxazoline). *Macromolecules,* 38(6), 2043-2046.

Yi, Y., Lin, G., Chen, S., Liu, J., Zhang, H., & Mi, P. (2018). Polyester micelles for drug delivery and cancer theranostics: Current achievements, progresses and future perspectives. *Mater Sci Eng C Mater Biol Appl,* 83, 218-232.

You, Y. Z., Hong, C. Y., Wang, W. P., Lu, W. Q., & Pan, C. Y. (2004). Preparation and characterization of thermally responsive and biodegradable block copolymer comprised of PNIPAAM and PLA by combination of ROP and RAFT methods. *Macromolecules,* 37(26), 9761-9767.

Yuan, W., Yuan, J., Zhang, F., & Xie, X. (2007). Syntheses, characterization, and in vitro degradation of ethyl cellulose-graft-poly(epsilon-caprolactone)-block-poly(L-lactide) copolymers by sequential ring-opening polymerization. *Biomacromolecules,* 8(4), 1101-1108.